

Jyoti Faujdar and Atul Kumar\*

# Analysing the Efficiencies of Partially Entangled Three-Qubit States for Quantum Information Processing Under Real Conditions

<https://doi.org/10.1515/zna-2018-0521>

Received November 26, 2018; accepted February 5, 2019

**Abstract:** In this article, we revisit the question of analysing the efficiencies of partially entangled states in three-qubit classes under real conditions. Our results show some interesting observations regarding the efficiencies and correlations of partially entangled states. Surprisingly, we find that the efficiencies of many three-qubit partially entangled states exceed that of maximally entangled three-qubit states under real noisy conditions and applications of weak measurements. Our analysis, therefore, suggests that the efficiencies of partially entangled states are much more robust to noise than those of maximally entangled states at least for the GHZ (Greenberger–Horne–Zeilinger) class states, for certain protocols; i.e. less correlations in the initially prepared state may also lead to better efficiency and hence one need not always consider starting with a maximally entangled state with maximum correlations between the qubits. For a set of partially entangled states, we find that the efficiency is optimal, independent of the decoherence and state parameters, if the value of weak measurement parameter is very large. For other values of the weak measurement parameter, the robustness of the states depends on the decoherence and state parameters. Moreover, we further show that one can achieve higher efficiencies in a protocol by using non-optimal weak measurement strengths instead of optimal weak measurement strengths.

**Keywords:** Nonlocal Correlations; Nonlocality; Teleportation.

## 1 Introduction

Quantum entanglement – shared between distant users – is shown to be an efficient resource in comparison to

its classical counterparts for many communication protocols such as quantum computing [1], quantum cryptography [2], quantum teleportation [3], dense coding [4], and quantum secret sharing [5]. The basic concept behind the efficiency of quantum resources in comparison to classical resources lies in the existence of long-range nonlocal correlations existing between the qubits [6–10]. These correlations, however, are subjected to decoherence due to the interaction of entangled qubits with the environment during entanglement distribution [11–13]; this leads to degradation of entanglement and non-violation of the Bell-type inequality [13–17]. Interestingly, there are instances where nonlocal correlations in a partially entangled state are found to be more robust in comparison to a maximally entangled state, leading to the anomaly [18, 19] that maximal nonlocality may not coincide with maximum entanglement [20–31]. These unavoidable couplings further result in the decreased efficiency of entangled resources in quantum information processing protocols. For example, in general, if an entangled resource used for quantum teleportation is maximally entangled or belongs to some specialised class, then one can achieve perfect teleportation with unit fidelity [32–34]. However, because of the interaction with the environment, a maximally entangled pure state may evolve into a mixed state, resulting in decreased fidelity of quantum teleportation [35]. Moreover, in comparison to a maximally entangled multi-qubit state, if the users in a communication protocol share a multi-qubit partially entangled state, then the fidelity of teleportation depends on the parameters of the state to be teleported, even under ideal conditions [33, 36, 37]. Clearly, the situation becomes much more intricate when one considers a real experimental set-up where the noise cannot be ignored any longer; hence, the need to analyse the efficiency of partially entangled multi-qubit states under real noisy conditions so that one can take informed decisions whether to use a particular entangled state under noisy conditions or not. One of the measures to compare the efficiencies of entangled states is the fidelity of teleportation. For example, quantum teleportation is considered to be successful for fidelity  $> \frac{2}{3}$  [38–40]. Since the channel capacity also depends on the degree of entanglement between the qubits, states leading to fidelity  $\leq \frac{2}{3}$  cannot be used as efficient resources for

\*Corresponding author: Atul Kumar, Indian Institute of Technology Jodhpur, Rajasthan, India, E-mail: atulk@iitj.ac.in

Jyoti Faujdar: Indian Institute of Technology Jodhpur, Rajasthan, India

quantum teleportation. The influence of noisy channels on the teleportation protocol using maximally and partially entangled multi-qubit Greenberger–Horne–Zeilinger (GHZ) and  $W$  states have been studied [35, 41, 42]. Thus, noisy channels impact teleportation fidelity adversely so that the fidelity may become  $\leq \frac{2}{3}$ , and therefore one needs to find other ways to protect quantum coherence between qubits in a communication scenario under real conditions. Similarly, in a dense coding protocol, the channel capacity to transmit classical information can be considered as a criterion for examining the usefulness of a state [43]. Although there are many decoherence models to protect the required coherence [44–48], the one that is proved to be very useful is weak measurement and its reversal operations [49–61]. This model is based on the fundamental possibility of reversing partial measurement operations. Recently, the strategy to use weak measurement and its reversal operation was shown to be very useful in quantum information and computation, theoretically as well as experimentally [58–65]. For example, the teleportation fidelity of a two-qubit shared state can be increased by the applications of weak measurement and its reversal operation [66]. Such analysis for multi-qubit entangled systems may provide a better insight into the complex nature of nonlocal correlations as well as the usefulness and efficiencies of these resources. Hence, it will be interesting to analyse the robustness of efficiencies of partially entangled three-qubit states under noisy conditions to understand the range of different parameters involved in the process for achieving maximum efficiency.

We, therefore, readdress the question of the usefulness and efficiency of multi-qubit, partially entangled states under real noisy conditions using weak measurement and its reversal operations. For this purpose, we analyse and compare the efficiencies of three different sets of three-qubit, partially entangled states from two inequivalent classes, namely the GHZ class and the  $W$  class [67], for teleportation and dense coding protocols. Our analysis shows some interesting observations regarding the applications of weak measurement and its reversal operations for amplitude damping channels. For instance, using a class of states ( $|\Phi\rangle$ ) belonging to the GHZ class as a resource for quantum teleportation, we find that fidelity of teleportation is always close to unity for higher values of the weak measurement strength parameter irrespective of the strength of the noise parameter and the state parameter  $\theta$ . For GHZ and  $W$  classes of states, applications of weak measurements leads to an increase in the fidelity of teleportation compared to that in the presence of noise alone. A comparison of our results suggests that, for lower values of the state parameter  $\theta$ , the  $|\Phi\rangle$  states are

much more robust to decoherence in comparison to other generalised GHZ (GGHZ) states, whereas for higher values of  $\theta$ , the GGHZ states are more robust to decoherence in comparison to the  $|\Phi\rangle$  states. In general,  $|\Phi\rangle$  and GGHZ states are always more robust to noise in comparison to  $W$  states. However, using the weak measurement technique, our results suggest that for lower values of the weak measurement parameter (say 0.2) and moderate noise (0.5), the use of standard  $W$  states [ $\theta = 35.2644^\circ$ ; (13)] leads to better efficiency than the use of  $|\Phi\rangle$  or GHZ states at the same  $\theta$ . Similar to the anomaly shown in nonlocality characterisation [18, 19, 25, 27, 28], where maximal nonlocality does not coincide with maximum entanglement, our analysis further shows that the maximum efficiency also does not coincide with the maximum entanglement; i.e. partially entangled states turn out to be more efficient than a maximally entangled state at least in the analysis of  $|\Phi\rangle$  and GGHZ states. The observations regarding the efficiency of dense coding protocol are also in agreement with the discussions regarding the efficiency of teleportation in the presence of noise and weak measurement. All the above description of efficiencies of partially entangled three-qubit states is obtained using an optimal relation between the weak measurement parameter, the weak measurement reversal parameter, and the decoherence parameter. Interestingly, we find that, under the application of non-optimal reversing weak measurement, for a fixed value of the decoherence parameter, the partially entangled GGHZ states are more efficient for quantum information protocols than all other states of the same class, for certain values of weak measurement operations. For example, at a decoherence parameter value of 0.5, if we fix the value of the weak measurement reversal parameter as 0.99, then the use of partially entangled GGHZ states as resources results in very high average teleportation fidelity at very small values of the state parameter,  $\theta \in [0.003, 0.4]$ , for all values of weak measurement strength below 0.98. Therefore, our results indicate that states with less initial correlations may prove to be more useful in comparison to states with higher initial correlations under noisy conditions, confirming that higher initial correlations may not always guarantee higher success in a communication protocol. Hence, the efficiency of a set of states depends on different parameters, i.e. the state parameter, the noise parameter, weak measurement, and its reversal operations (optimal and non-optimal). The values of these parameters decide whether to use a  $|\Phi\rangle$  or a GGHZ class state in real conditions. Thus, based on the analysis presented in this article, one can use an appropriate state as a resource in an actual protocol set-up to obtain maximum efficiency. We believe that the study presented

here will be useful to researchers working in theory as well as experiments.

For characterizing the quantum correlations in the finally shared three-qubit states, we use the three-qubit Svetlichny inequality [68] whose violation is a necessary and sufficient condition to confirm the presence of non-local correlations in an underlying quantum state. Our results indicate that, although the Svetlichny inequality is not violated by three-qubit, partially entangled states even for a small decoherence parameter, the fidelity of teleportation is surprisingly greater than  $\frac{2}{3}$ . A further comparison of the efficiencies of these states for dense coding protocol under similar scenarios leads to similar results as in the case of teleportation protocol, i.e.  $|\Phi\rangle$  states are found to be more efficient in comparison to GHZ states for smaller values of the state parameter  $\theta$ , and  $|\Phi\rangle$  and GHZ states are always more efficient than  $W$  states. For understanding the reasons behind the efficiency of these states for teleportation and dense coding even when the Svetlichny inequality is not violated, we further analyse the global quantum discord [69] to explain the robustness of nonlocal correlations under the influence of noise.

In following sections, we first briefly discuss decoherence, weak measurement, its reversal operations, and nonlocal correlations in three-qubit systems, and then move ahead to analyse the efficiencies of three-qubit, partially entangled states for quantum information processing.

## 2 System-Environment Interactions

In any communication protocol, system qubits always interact with the environment, leading to unwanted coupling and resulting in noise [11]. The coupling of system qubits with the environment is described as the evolution  $\varepsilon(\rho)$  of the density operator  $\rho$  by the completely positive trace-preserving evolution

$$\varepsilon(\rho) = \sum_k E_k \rho E_k^\dagger,$$

where  $E_k = \langle k|U|0\rangle$  are single-qubit Kraus operators represented as

$$E_0 = \begin{bmatrix} 1 & 0 \\ 0 & \sqrt{1-d} \end{bmatrix}, \quad E_1 = \begin{bmatrix} 0 & \sqrt{d} \\ 0 & 0 \end{bmatrix} \quad (1)$$

and  $d$  is the decoherence parameter ( $0 \leq d \leq 1$ ). The operational elements  $E_k$  describe the interaction of the system qubits with the environment and satisfy the relation  $\sum_k E_k^\dagger E_k = I$ . Since decoherence affects the correlation between qubits, it is evident that efficiency of teleportation protocol also gets affected under noisy conditions [70, 71].

## 3 Weak Measurement and Quantum Measurement Reversal Operations

In 2012, Kim et al. [59] proposed a scheme to protect entanglement from decoherence, based on the fact that weak measurements can be reversed. The proposed scheme makes use of weak measurement and the corresponding quantum measurement reversal to avoid the effect of decoherence, as shown in Figure 1, where  $w$  is the weak measurement strength,  $d$  is decoherence parameter, and  $w_r$  is the strength of the reversing measurement. For an amplitude damping channel, the optimum value for the reversal measurement is given as  $w_r = w + d(1-w)$  [59]. The individual qubits undergoing decoherence are first subjected to weak measurement operations locally before being distributed through a decoherence channel and, then, after the decoherence channel, quantum measurement reversal operations are performed on the respective qubits. The whole scenario allows one to protect quantum entanglement and nonlocal correlations between the qubits and hence is useful for many quantum information and computation tasks.

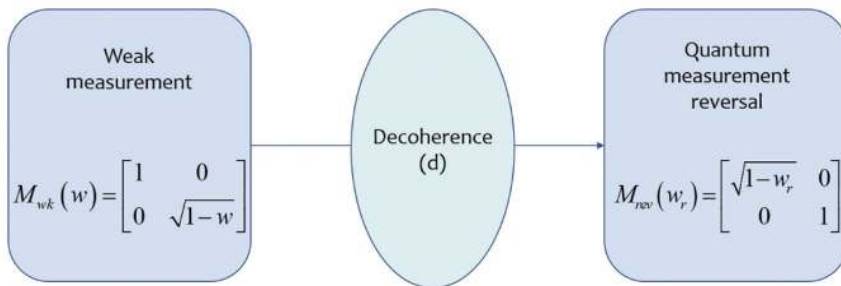


Figure 1: Application of weak measurement and quantum measurement reversal in the decoherence channel.

## 4 Nonlocal Correlations

Quantum theory allows correlations between spatially separated particles, which are fundamentally different from classical correlations. For example, the violation of Bell-type inequalities in bipartite and multi-qubit entangled systems confirms the presence of genuine quantum correlations between the particles. These correlations, when subjected to noisy quantum channels, degrade as a result of decoherence, affecting the overall efficiency of a protocol. In this article, we emphasise on analysing such nonlocal correlations and efficiency of three-qubit partially entangled states.

For three-qubit systems, the violation of the Svetlichny inequality [68] is defined as follows:

$$|S| = A(BC + BC' + B'C + B'C') + A'(BC + BC' + B'C + B'C') \leq 4, \quad (2)$$

where  $A = \vec{a} \cdot \vec{\sigma}_a$  or  $A' = \vec{a}' \cdot \vec{\sigma}_a$  are measurements performed on the first sub-system; similarly,  $B = \vec{b} \cdot \vec{\sigma}_b$  or  $B' = \vec{b}' \cdot \vec{\sigma}_b$  and  $C = \vec{c} \cdot \vec{\sigma}_c$  or  $C' = \vec{c}' \cdot \vec{\sigma}_c$  are for second and third sub-systems, respectively. Here,  $\vec{\sigma}_i = \{\sigma_x, \sigma_y, \sigma_z\}$  (with  $i = a, b, c$ ) are the spin projection operators, and  $\vec{a}, \vec{b}, \vec{c}, \vec{a}', \vec{b}', \vec{c}'$  are unit vectors in  $\mathbb{R}^3$ , given as  $\vec{a} = (\sin \theta_a \cos \phi_a, \sin \theta_a \sin \phi_a, \cos \theta_a)$ ; similarly,  $\vec{b}, \vec{c}$  with angles corresponding to sub-systems  $b$  and  $c$  and  $\vec{a}', \vec{b}', \vec{c}'$  with prime angles.

The Svetlichny inequality confirms the presence of genuine tripartite correlations between the qubits. In general, the violation of the Svetlichny inequality, therefore, suggests that the underlying quantum state can be used as an efficient resource in quantum information processing. For example, the Svetlichny inequality is violated by the state  $|\Phi\rangle = \frac{1}{\sqrt{2}}[\cos \theta(|000\rangle + |011\rangle) + \sin \theta(|110\rangle + |101\rangle)]$  for the whole range of the parameter  $\theta$  or by the set of GGHZ states, i.e.  $|\text{GGHZ}\rangle = \cos \theta|000\rangle + \sin \theta|111\rangle$  for  $\theta > 0.4$  rad, and hence  $|\Phi\rangle$  and GGHZ states can be considered as useful resources for quantum information and computation. However, as shown in Figure 2, the inequality is not violated by the  $|\Phi\rangle$  states if the decoherence parameter is as small as 0.2. In fact, even for the value  $d = 0.1$ , the inequality is violated only for a smaller set of states. Figure 2 therefore suggests that, although the  $|\Phi\rangle$  states always violate the Svetlichny inequality in ideal conditions, the nonlocal correlations in these states degrade very fast when exposed to real conditions. Similar to the  $|\Phi\rangle$  states, the GGHZ states do not violate the inequality if the decoherence parameter is greater than 0.2. Precisely, for the value of decoherence parameter as small as 0.2 itself, only a fraction of states violate the

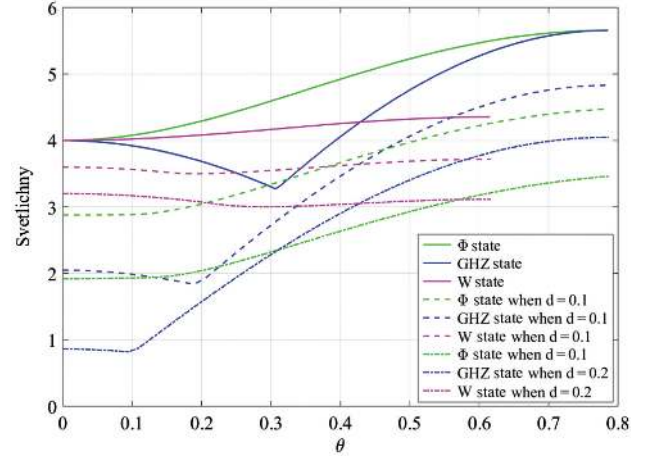


**Figure 2:** Effect of decoherence on quantum correlations using the Svetlichny inequality for  $|\Phi\rangle$ , GGHZ, and  $W$  states.

Svetlichny inequality. Interestingly, for  $d = 0.1$ , the violation of the Svetlichny inequality by the GGHZ states is more prominent than the  $|\Phi\rangle$  states; i.e. although  $|\Phi\rangle$  states violate the Svetlichny inequality more in comparison to the GGHZ states under ideal conditions, the GGHZ states exhibit more nonlocal correlations in comparison to the  $|\Phi\rangle$  states under mild noisy conditions (see Fig. 2). In comparison to the GGHZ and  $|\Phi\rangle$  states, the  $W$  states, i.e.  $|W\rangle = \sin \theta|001\rangle + \cos \theta(|100\rangle + |010\rangle)/\sqrt{2}$ , do not reveal the presence of nonlocal correlations even at  $d = 0.1$ . Considering the vulnerability of nonlocal correlations even towards mild noise, the analysis of efficiency of such states under real noisy conditions requires adequate attention. Hence, in the next few sections we analyse the efficiencies of partially entangled three-qubit states under real conditions.

## 5 Quantum Teleportation using Quantum Gates

Quantum teleportation [3] is a process by which quantum information can be transmitted from one location to another, without travelling the distance physically, with the help of previously shared entanglement between a sender and a receiver. In order to facilitate the discussion regarding our results, we first briefly describe quantum teleportation: Alice (sender) and Bob (receiver) share an entangled state  $|\psi_{23}^-\rangle$ , which acts as a quantum channel for the teleportation protocol. Alice wants to send an unknown information encoded in a state  $|\psi_{in}\rangle = \cos(\xi/2)|0\rangle + e^{i\phi} \sin(\xi/2)|1\rangle$  to Bob, where  $\xi$  and  $\phi$  are polar coordinates with  $0 \leq \xi \leq \pi$  and  $0 \leq \phi \leq 2\pi$ . For

this, Alice first performs a two-qubit Bell-state measurement on the joint state of her qubits, one from the shared entangled pair and one defining the input state, and then sends the measurement outcomes to Bob through a classical channel. Bob then performs a unitary transformation to retrieve the unknown input state, which is destroyed at Alice's end.

As a criterion for successful teleportation, one can compute the teleportation fidelity, which indicates the degree of overlap between the input and output states. For example, fidelity of quantum teleportation can be expressed as the overlap of the input state  $|\psi_{in}\rangle$  and the output state  $\rho_{out}$  as

$$F = \langle \psi_{in} | \rho_{out} | \psi_{in} \rangle. \quad (3)$$

Since the initial state is unknown, the average fidelity [72] can also be given as

$$F_{avg} = \frac{1}{4\pi} \int_0^{2\pi} d\phi \int_0^{\pi} F \sin(\xi) d\xi. \quad (4)$$

## 5.1 Three-Qubit States as Quantum Channels for Teleportation Under Real Conditions

In order to analyse the efficiencies of partially entangled multi-qubit states in terms of teleportation fidelity in a noisy environment, we now proceed to study three different sets of three-qubit states belonging to two inequivalent classes. As discussed above, for our purpose we consider three different sets of states, namely,  $|\Phi\rangle$  states, GHZ states, and  $W$  states.

### 5.1.1 $|\Phi\rangle$ State as a Quantum Channel Under Real Conditions

First, we consider the partially entangled  $|\Phi\rangle$  states as a channel for teleportation protocol, where

$$|\Phi\rangle = \frac{1}{\sqrt{2}} [\cos \theta (|000\rangle + |011\rangle) + \sin \theta (|110\rangle + |101\rangle)]. \quad (5)$$

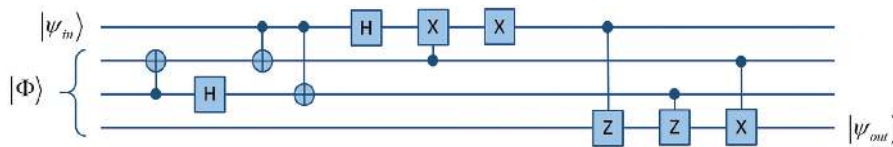


Figure 3: Teleportation using the  $|\Phi\rangle$  state as a quantum channel.

As a preliminary example, in Figure 3 we show a quantum circuit for teleporting an unknown information encoded in the state  $|\psi_{in}\rangle = \alpha|0\rangle + \beta|1\rangle$ , where  $\alpha$  and  $\beta$  are real numbers, using the  $|\Phi\rangle$  state as a quantum channel under ideal conditions. Here  $H$ ,  $X$ , and  $Z$  represent the Hadamard, Pauli X, and Pauli Z operations, respectively, and the two-qubit operations are Controlled-NOT (C-NOT) and Controlled-Z operations.

Using the teleportation circuit diagram in Figure 3,  $|\psi_{out}\rangle$  can be evaluated as

$$|\psi_{out}^{(1)}\rangle = \frac{1}{2\sqrt{2}} \left( \frac{(\cos \theta + \sin \theta)(\alpha|0\rangle + \beta|1\rangle)}{\sqrt{p(\psi_{out}^{(1)})}} \right)$$

or

$$|\psi_{out}^{(2)}\rangle = \frac{1}{2\sqrt{2}} \left( \frac{(\cos \theta - \sin \theta)(\alpha|0\rangle + \beta|1\rangle)}{\sqrt{p(\psi_{out}^{(2)})}} \right)$$

for measurement outcomes corresponding to  $(000, 100, 011, 111)_{123}$  or  $(001, 101, 010, 110)_{123}$ , respectively. Considering  $p(\psi_{out}^{(i)})$  as the probabilities of measurement outcomes associated with the states  $|\psi_{out}^{(i)}\rangle$ , we have  $p(\psi_{out}^{(1)}) = \frac{1}{8}(\cos \theta + \sin \theta)^2$  and  $p(\psi_{out}^{(2)}) = \frac{1}{8}(\cos \theta - \sin \theta)^2$ . Therefore, using (3), fidelity can be calculated as

$$F^{(1)} = \frac{1}{8} \left( \frac{(\alpha^2 + \beta^2)^2 (\cos \theta + \sin \theta)^2}{p(\psi_{out}^{(1)})} \right)$$

and

$$F^{(2)} = \frac{1}{8} \left( \frac{(\alpha^2 + \beta^2)^2 (\cos \theta - \sin \theta)^2}{p(\psi_{out}^{(2)})} \right).$$

Hence, the average fidelity  $F_{avg} = \sum_i p(\psi_{out}^{(i)}) F^{(i)}$ , using the above teleportation circuit, can be given as

$$\begin{aligned} F_{avg} &= \frac{1}{2} [(C_\theta + S_\theta)^2 + (C_\theta - S_\theta)^2] (\alpha^2 + \beta^2)^2 \\ &= 1, \end{aligned} \quad (6)$$

where  $C_\theta = \cos \theta$  and  $S_\theta = \sin \theta$ . Clearly, the average teleportation fidelity in this case is found to be 1, indicating

perfect teleportation and showing that the fidelity of teleportation is independent of the state parameter  $\theta$ . We now proceed to discuss the main results of this article considering the actual teleportation protocol in a decoherence environment, i.e. using amplitude damping channels. The single-qubit amplitude damping Kraus operators, defined in (1), operate on the individual qubits such that the state now evolves as  $\varepsilon(\rho)$ . Since the initial state after operations of amplitude damping channels evolves as a mixed state, the input state in Figure 3 is now a three-qubit mixed state instead of a three-qubit pure state. Considering all three qubits of the state  $|\Phi\rangle$  to suffer from decoherence, the average fidelity can be expressed as

$$F_{\text{avg}} = \frac{1}{6} \{4 + 2\sqrt{\bar{d}_2}\sqrt{\bar{d}_3} - d_2\bar{d}_3 - d_3\bar{d}_1 + d_1(-\bar{d}_2 - 2\sqrt{\bar{d}_2}\sqrt{\bar{d}_3}) + (2d_1\sqrt{\bar{d}_2}\sqrt{\bar{d}_3} + d_2d_3 + d_1(\bar{d}_2 - d_3))C_{2\theta}\}, \quad (7)$$

where  $d_1$ ,  $d_2$ , and  $d_3$  are the amplitude damping parameters associated with qubits 1, 2, and 3, respectively

( $0 \leq d_1 \leq 1$ ,  $0 \leq d_2 \leq 1$ , and  $0 \leq d_3 \leq 1$ ) and  $\bar{d}_i = 1 - d_i$ . Equation (7) indicates that the teleportation fidelity decreases with increasing values of the amplitude damping parameter (see Fig. 4a). Surprisingly, in this case, the teleportation fidelity using the finally shared state is always more if the initially prepared state is a partially entangled state instead of a maximally entangled state. Evidently, the lesser the entanglement of the initial state, the more the teleportation fidelity. Therefore, the partially entangled  $|\Phi\rangle$  states are more robust towards amplitude damping noise in comparison to the maximally entangled  $|\Phi\rangle$  state. The above observation is in correspondence with the fact that maximally entangled states may not give rise to maximum nonlocality for some seemingly good nonlocality measures [18–26]. The results obtained here therefore point towards the anomaly that maximal nonlocality does not coincide with maximum entanglement for the three-qubit Svetlichny inequality. In fact, for very strong decoherence, the maximally entangled state may not even lead to a fidelity  $> \frac{2}{3}$  as shown in Figure 4a and b. Hence, more nonlocal correlations in the initial

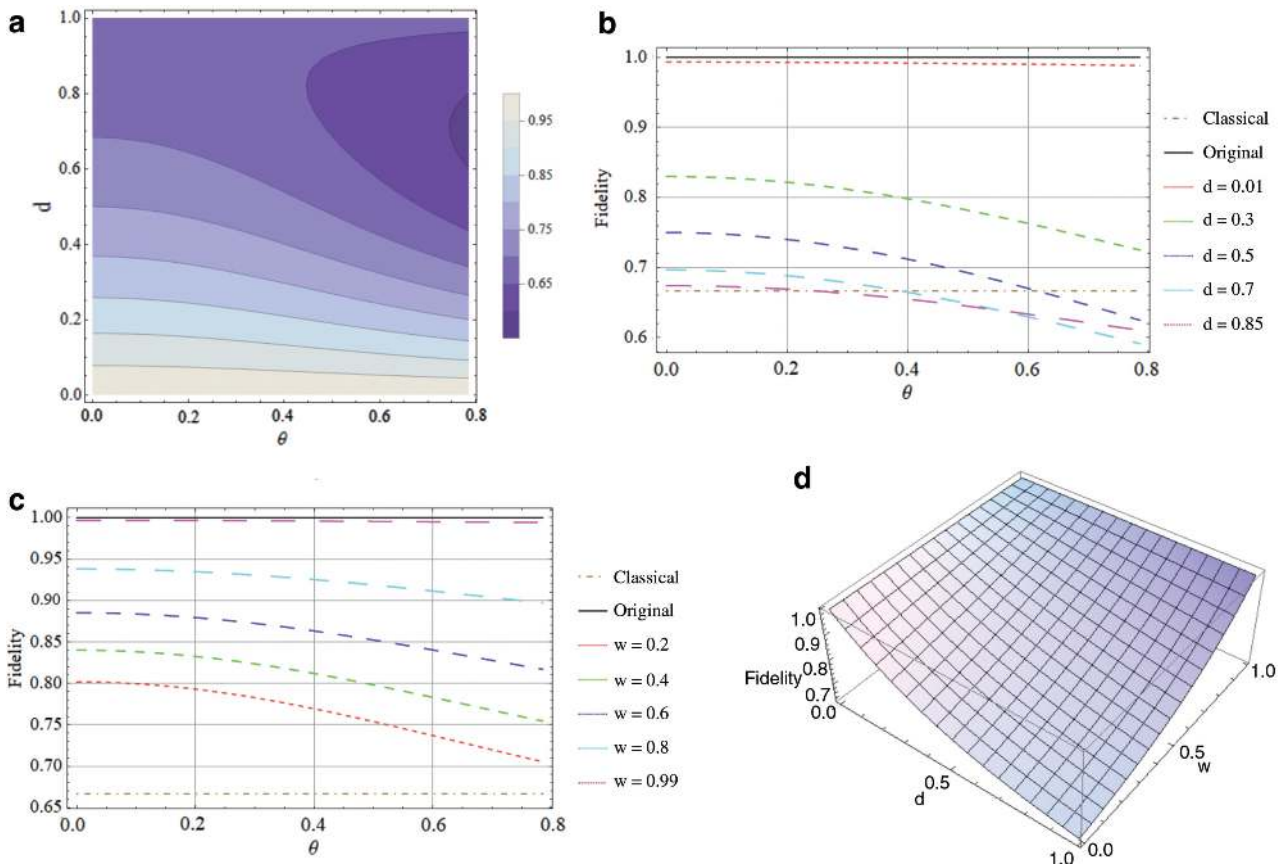


**Figure 4:** Effect of decoherence and weak measurement on the  $|\Phi\rangle$  states: (a) and (b) represent the loss of teleportation fidelity when all three qubits of the  $|\Phi\rangle$  states undergo decoherence ( $d_1 = d_2 = d_3 = d$ ); (c) represents improving teleportation fidelity in decoherence environment ( $d = 0.5$ ) using weak measurement on all three qubits of the  $|\Phi\rangle$  state ( $w_1 = w_2 = w_3 = w$ ); (d) represents the effect of decoherence and weak measurement on the  $|\Phi\rangle$  state when  $\theta = \frac{\pi}{8}$ .

state do not always guarantee more success in a given protocol. Another interesting observation is that, even though the  $|\Phi\rangle$  states do not violate the three-qubit Svetlichny inequality for  $d \geq 0.2$ , the fidelity of teleportation using these states is still  $> \frac{2}{3}$  for  $d \geq 0.2$ . Even for strong decoherence parameter values, fidelity is still  $> \frac{2}{3}$  for certain ranges of the parameter  $\theta$ . We further analyse the efficiency of the  $|\Phi\rangle$  states using the application of weak measurement and its reversal operations as depicted in Figure 1. The average teleportation fidelity after a sequence of weak measurements, amplitude damping channels, and quantum measurement reversal operations is evaluated as

$$F_{\text{avg}} = \frac{2}{3} \left[ \frac{6 + d_3 \bar{w}_3 (1 + d_1 \bar{w}_1) + d_2 \bar{w}_2 (1 + d_1 \bar{w}_1 + d_3 \bar{w}_3) - (d_1 \bar{w}_1 (d_2 \bar{w}_2 + d_3 \bar{w}_3) - d_2 d_3 \bar{w}_2 \bar{w}_3) C_{2\theta}}{(2 + d_2 \bar{w}_2)(2 + d_3 \bar{w}_3) + d_1 \bar{w}_1 (2 + d_2 \bar{w}_2 + d_3 \bar{w}_3) - (d_1 \bar{w}_1 (2 + d_2 \bar{w}_2 + d_3 \bar{w}_3) - d_2 d_3 \bar{w}_2 \bar{w}_3) C_{2\theta}} \right] \quad (8)$$

where  $w_1, w_2, w_3$  are the weak measurement parameters on qubits 1, 2, and 3, respectively ( $0 \leq w_1 \leq 1, 0 \leq w_2 \leq 1, \text{ and } 0 \leq w_3 \leq 1$ ), and  $\bar{w}_i = 1 - w_i$ . Figure 4c demonstrates the effect of weak measurement and its reversal operations on the average fidelity of teleportation under noisy conditions, considering  $d = 0.5$ . Comparison of Figure 4b and c confirms the enhancement in teleportation fidelity at  $d = 0.5$  for the value of weak measurement strength  $w > 0.2$ . Remarkably, for larger values of the weak measurement strength parameter, the fidelity approaches unity independent of the strengths of decoherence and the state parameters. Therefore, these states can be used as efficient resources even in the presence of very strong noise. Moreover, fidelity is always greater than  $\frac{2}{3}$  even at higher decoherence values where the Svetlichny inequality is not violated by the  $|\Phi\rangle$  states. From Figure 4c and d, one can conclude that partially entangled states  $|\Phi\rangle$  are still more robust to decoherence under the applications of weak measurement and its reversal operations. In order to understand the reasons behind fidelity being  $> \frac{2}{3}$  even at high decoherence where the  $|\Phi\rangle$  states fail to violate the Svetlichny inequality, we use global quantum discord [69] to capture nonlocal correlations in the finally shared three-qubit mixed states. The quantum discord  $D(\rho)$  for an arbitrary three-qubit state  $\rho_{ABC}$  under a set of local measurements  $\{\Pi^k\}$  is defined as

$$D(\rho) = \min_{\{\Pi^k\}} [S(\rho|\phi(\rho)) - S(\rho_A|\phi_A(\rho_A)) - S(\rho_B|\phi_B(\rho_B)) - S(\rho_C|\phi_C(\rho_C))], \quad (9)$$

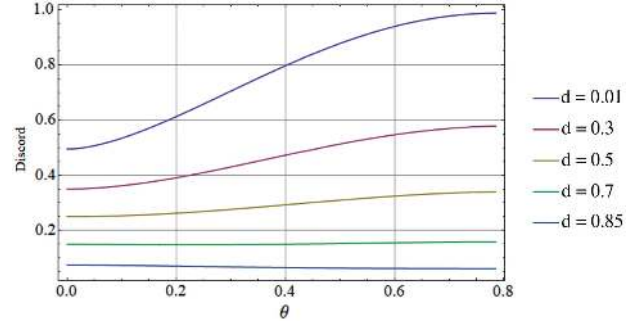


**Figure 5:** Effect of decoherence on quantum correlations using discord for the  $|\Phi\rangle$  state.

where  $\phi_i(\rho_i) = \sum_k \Pi^k \rho_i \Pi^k$  and  $S(\rho)$  is von-Neumann entropy of the state  $\rho$ .

Figure 5 confirms that correlations in the  $|\Phi\rangle$  states are much more robust in the presence of decoherence as against the indication given by the Svetlichny inequality. The characterisation of nonlocal correlations using discord, therefore, justifies the efficiency of the  $|\Phi\rangle$  states in quantum teleportation under real conditions.

### 5.1.2 GGHZ State as a Quantum Channel Under Real Conditions

In this section, we consider the GGHZ states given by

$$|\text{GGHZ}\rangle = \text{Cos } \theta |000\rangle + \text{Sin } \theta |111\rangle. \quad (10)$$

The quantum circuit for teleporting a single qubit using the GGHZ state as a quantum channel is shown in Figure 6. Unlike the  $|\Phi\rangle$  states, the average teleportation fidelity using the GGHZ states as resources in ideal conditions depends on the state parameter  $\theta$ , i.e.  $F_{\text{avg}} = \frac{1}{3} [2 + \text{Sin}(2\theta)]$ , which is the same as in [32].

Similarly, the average teleportation fidelity under the influence of amplitude damping noise and after the application of weak measurement and its reversal operations can be evaluated as

$$F_{\text{avg}} = \frac{1}{6} \{4 - (d_2 + d_3 - 2d_2 d_3)(1 - C_{2\theta}) + 2\sqrt{\bar{d}_1} \sqrt{\bar{d}_2} \sqrt{\bar{d}_3} S_{2\theta}\} \quad (11)$$

and

$$F_{\text{avg}} = \frac{(1 + d_1 \bar{w}_1)(2 + d_3 \bar{w}_3 d_2 \bar{w}_2 (1 + 2d_3 \bar{w}_3)) S_\theta^2}{3(C_\theta^2 + (1 + d_1 \bar{w}_1)(1 + d_2 \bar{w}_2)(1 + d_3 \bar{w}_3) S_\theta^2)} + \frac{2C_\theta^2 + S_{2\theta}}{3(C_\theta^2 + (1 + d_1 \bar{w}_1)(1 + d_2 \bar{w}_2)(1 + d_3 \bar{w}_3) S_\theta^2)}, \quad (12)$$

respectively.

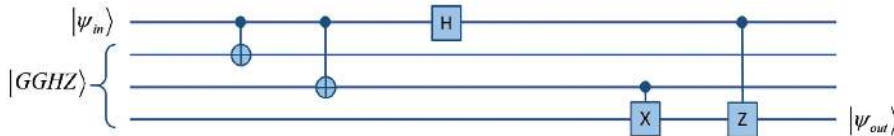


Figure 6: Teleportation using the GHZ state as a quantum channel.

Figure 7a–d depict the effect of the amplitude damping channel and weak measurement and its reversal operations on teleportation fidelity. Similar to the previous case, we observe that weak measurement and its reversal operations increase the teleportation fidelity for a given decoherence channel. In fact, for higher values of weak measurement strength, one can achieve fidelity equal to that in the ideal scenario. On the other hand, unlike the previous case, the maximally entangled states are found to be more robust under the influence of mild decoherence in comparison to partially entangled states. Interestingly, for higher decoherence, the robustness of partially entangled states increases with increase in the degree of entanglement and then decreases as one approaches the

maximally entangled states, further suggesting the presence of the anomaly as discussed in the previous subsection. For a fixed noise parameter, similar observations can be obtained as one decreases the value of weak measurement strengths. Therefore, the behaviours of two sets of states  $|\Phi\rangle$  and GHZ towards noise and weak measurements are different from each other. A comparison of our results for efficiencies of the  $|\Phi\rangle$  and GHZ states suggests that, for lower values of the state parameter  $\theta$ , the  $|\Phi\rangle$  states are more robust to decoherence in comparison to the GHZ states. The GHZ states, however, may prove to be a better resource in terms of teleportation fidelity for higher values of  $\theta$ . The above analysis further receives support from Figures 5 and 8, where the latter describes nonlocal

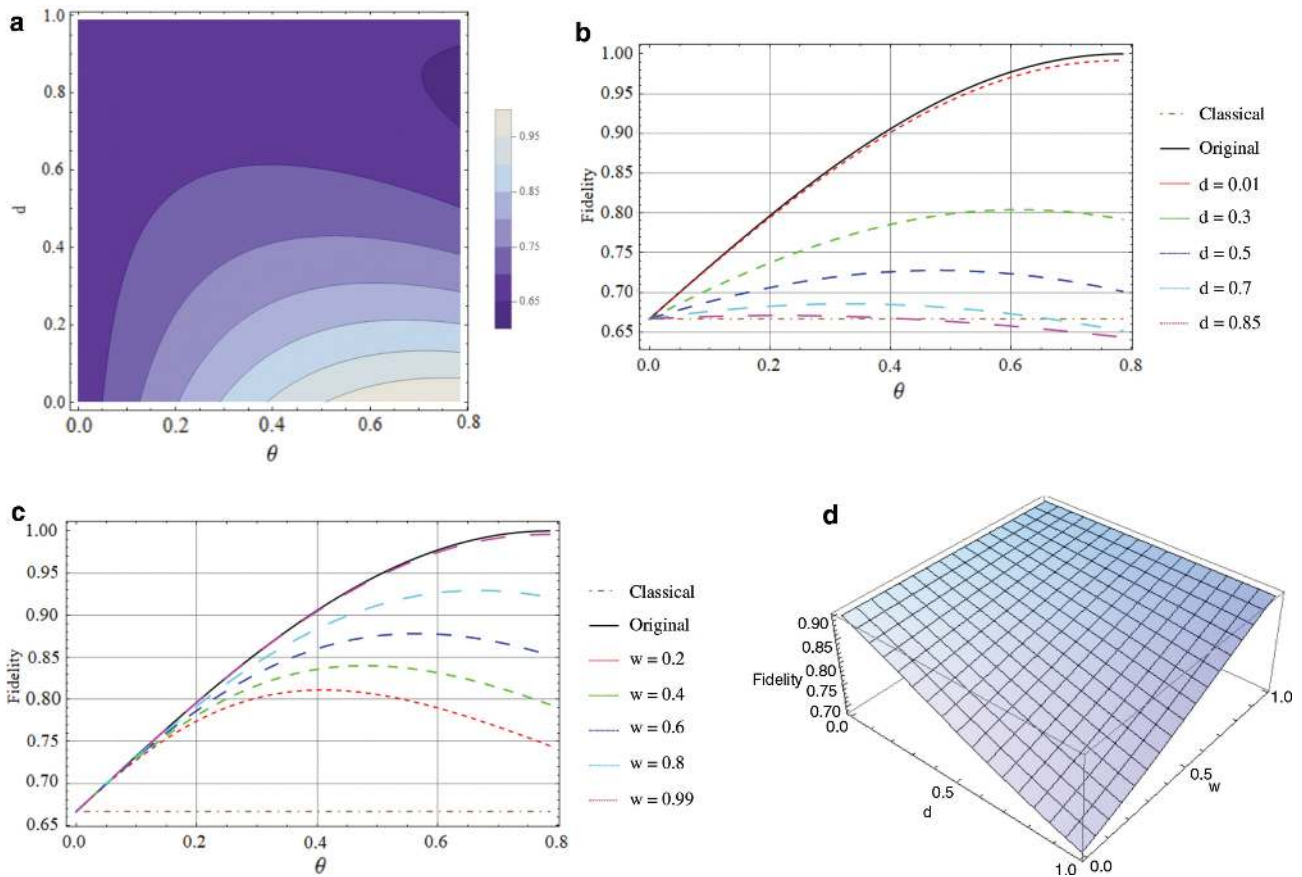
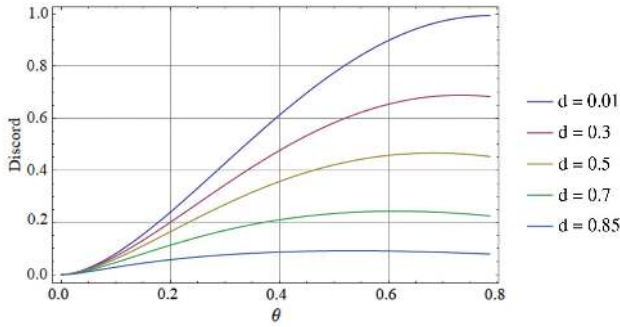


Figure 7: Effect of decoherence and weak measurement on GHZ states: (a) and (b) represent the loss of teleportation fidelity when all three qubits of GHZ states undergo decoherence ( $d_1 = d_2 = d_3 = d$ ); (c) represents improving teleportation fidelity in decoherence environment ( $d = 0.5$ ) using weak measurement on all three qubits of the GHZ state ( $w_1 = w_2 = w_3 = w$ ); (d) represents the effect of decoherence and weak measurement on the GHZ state when  $\theta = \frac{\pi}{8}$ .



**Figure 8:** Effect of decoherence on quantum correlations using discord for the GHZ state.

correlations in the originally prepared GHZ states under different values of the noise parameter.

### 5.1.3 $W$ state as a Quantum Channel Under Real Conditions

Finally, we consider another important class of three-qubit states as a quantum channel for teleportation, namely

$$|W\rangle = \sin \theta |001\rangle + \cos \theta (|100\rangle + |010\rangle) / \sqrt{2}, \quad (13)$$

where, if  $\theta = 35.2644^\circ$ , the state  $|W\rangle$  is a standard  $W$  state. In this case, Figure 9 describes the quantum circuit used for evaluating the average teleportation fidelity.

The quantum circuit in Figure 9 [35] is distinctly different from those used for the  $|\Phi\rangle$  and GHZ states. The unitary operation  $U$  is a three-qubit joint unitary operation and cannot be expressed in terms of the usual Pauli, Hadamard, and C-NOT operations, where  $U$  can be represented as

$$U = \frac{1}{2} \begin{bmatrix} 0 & 1 & 1 & 0 & \sqrt{2} & 0 & 0 & 0 \\ 0 & 0 & 0 & 2 & 0 & 0 & 0 & 0 \\ 0 & 0 & 0 & 0 & 0 & 0 & 0 & 2 \\ \sqrt{2} & 0 & 0 & 0 & 0 & 1 & 1 & 0 \\ 0 & 1 & 1 & 0 & -\sqrt{2} & 0 & 0 & 0 \\ 0 & \sqrt{2} & -\sqrt{2} & 0 & 0 & 0 & 0 & 0 \\ 0 & 0 & 0 & 0 & 0 & \sqrt{2} & -\sqrt{2} & 0 \\ \sqrt{2} & 0 & 0 & 0 & 0 & -1 & -1 & 0 \end{bmatrix}.$$

Similar to the case of the GHZ states, teleportation fidelity in this case also depends on the state parameter  $\theta$ ,

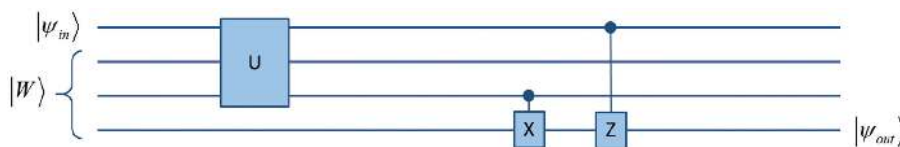


**Figure 9:** Teleportation using the  $W$  state as a quantum channel.

and can be given as  $\frac{1}{3}[2 + \sin(2\theta)]$ . As earlier, using the circuit diagram in Figure 9, the average teleportation fidelity under noisy conditions and after the application of weak measurement operations are

$$F_{\text{avg}} = \frac{1}{12} \{ (6 - d_1 - d_2 + 2\sqrt{d_1}\sqrt{d_2})C_\theta^2 - 4(-2 + d_3)S_\theta^2 + 2(\sqrt{d_1} + \sqrt{d_2})\sqrt{d_3}S_{2\theta} \} \quad (14)$$

and

$$F_{\text{avg}} = \frac{8 + d_1\bar{w}_1 + d_2\bar{w}_2 + 2d_3\bar{w}_3 + 4S_{2\theta}}{6((2 + d_1\bar{w}_1 + d_2\bar{w}_2)C_\theta^2 + 2(1 + d_3\bar{w}_3)S_\theta^2)} + \frac{(d_1\bar{w}_1 + d_2\bar{w}_2 - 2d_3\bar{w}_3)C_{2\theta}}{6((2 + d_1\bar{w}_1 + d_2\bar{w}_2)C_\theta^2 + 2(1 + d_3\bar{w}_3)S_\theta^2)}, \quad (15)$$

respectively.

In contrast to the cases of the  $|\Phi\rangle$  and GHZ states, teleportation fidelity of the initially prepared standard  $W$  state is always more than that of other initially prepared partially entangled states, as shown in Figure 10a and b, irrespective of the value of the noise parameter. Moreover, for  $d \geq 0.5$ , the set of  $W$  states are not useful for quantum teleportation. However, as depicted in Figure 10c, fidelity at  $d = 0.5$  can definitely be increased by the application of weak measurement and its reversal operations to achieve  $F_{\text{avg}} > \frac{2}{3}$  for certain ranges of the state parameter  $\theta$  depending on the value of the weak measurement parameter. Moreover, our results clearly demonstrate that the  $|\Phi\rangle$  and GHZ states are always more robust to noise as against the use of  $W$  states in absence of weak measurement and its reversal operations. However, for small values of the weak measurement parameter, we surprisingly find that the standard  $W$  state is more efficient than the  $|\Phi\rangle$  and GHZ states for the same value of the state parameter, i.e. at  $\theta = 35.2644^\circ$ . Although the range of  $\theta$  and weak measurement parameter is not very large for  $W$  states to be more efficient in comparison to the  $|\Phi\rangle$  and GHZ states, the result, nevertheless, is of high significance.

Figure 11 shows that the correlations identified by the discord (9) in the  $W$  states are much more robust in presence of decoherence as against the indication given by the Svetlichny inequality, which further rationalises the

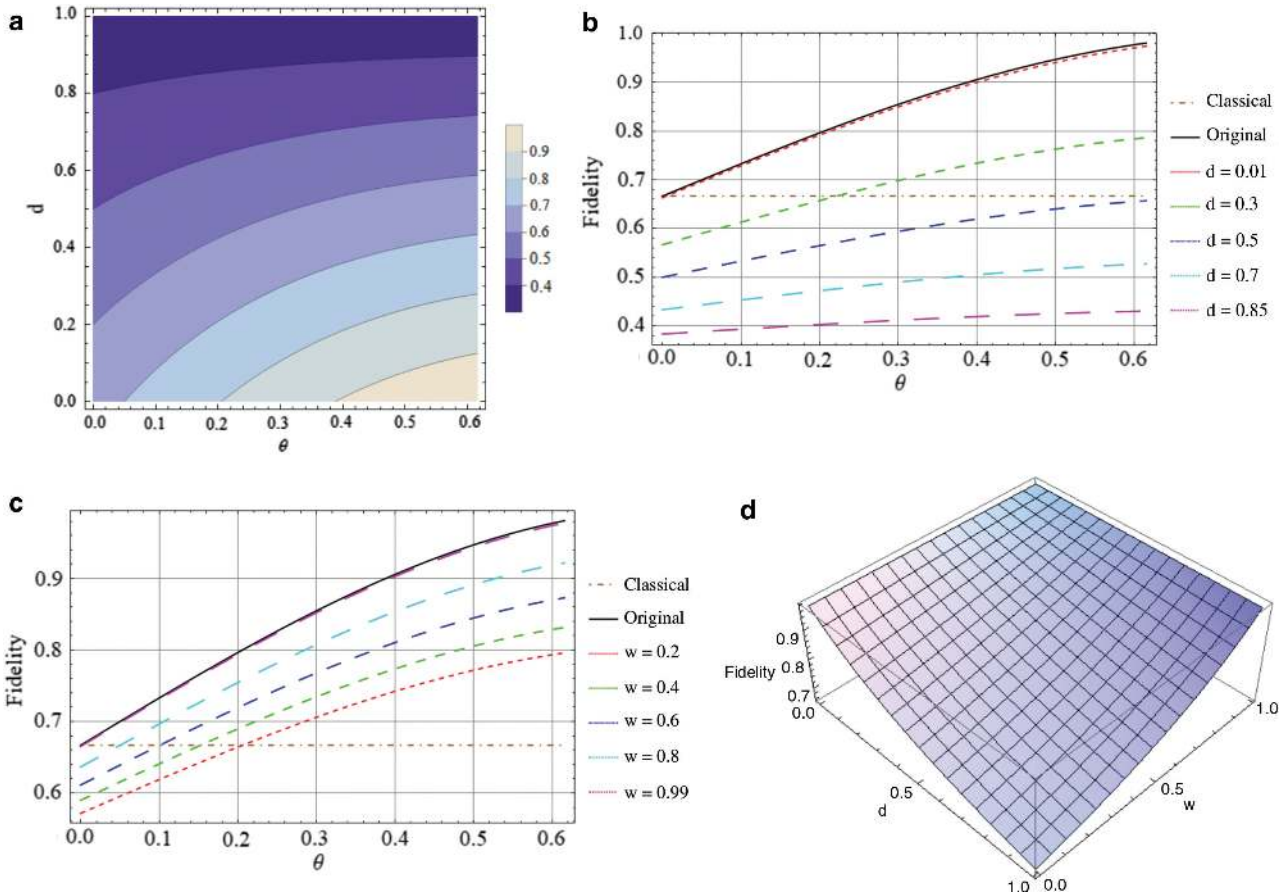


**Figure 10:** Effect of decoherence and weak measurement on  $W$  states: (a) and (b) represent the loss of teleportation fidelity when all three qubits of  $W$  states undergo decoherence ( $d_1 = d_2 = d_3 = d$ ); (c) represents improving teleportation fidelity in decoherence environment ( $d = 0.5$ ) using weak measurement on all three qubits of the  $W$  state ( $w_1 = w_2 = w_3 = w$ ); (d) represents effect of decoherence and weak measurement on the standard  $W$  state (i.e.  $\theta = 35.2644^\circ$  or  $0.6155$  rad).

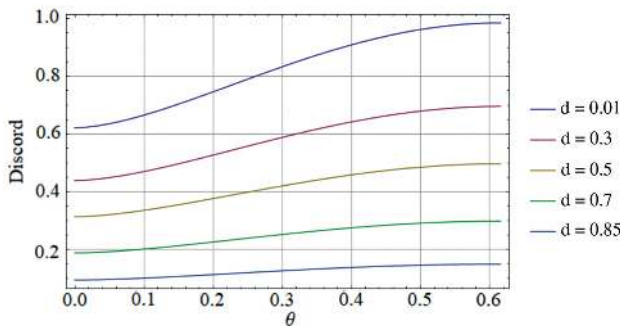


**Figure 11:** Effect of decoherence on quantum correlations using discord for the  $W$  state.

efficiency of the  $W$  states in quantum teleportation under noisy conditions.

## 6 Quantum Dense Coding

Bennett and Wiesner [4] realised one of the simplest applications of quantum entanglement in the form of a

dense coding protocol. In general, one can send one bit information classically from a sender to a receiver using a qubit. However, if the sender and receiver share a maximally entangled state of two qubits, then the sender can send two bits of classical message to the receiver using his/her one qubit. Therefore, the use of  $N$  pairs of maximally entangled two-qubit states results in the transmission of  $2N$  bits of information, thereby doubling the classical information capacity of a channel. In the superdense coding protocol, an entangled state is distributed between a sender and a receiver. The sender performs one of the four single-qubit unitary operations, i.e.  $I, \sigma_x, \sigma_{iy},$  and  $\sigma_z$ , corresponding to a prior agreed encoding information and then sends his/her qubit to the receiver, who in turn performs a two-qubit Bell-state measurement to decode the message.

The dense coding capacity [73] for a quantum system  $\rho_{AB}$  can be used as a measure of its efficiency to transmit classical information, and is given by

$$C = \log_2(D_A) + S(\rho_B) - S(\rho_{AB}), \quad (16)$$

where  $D_A$  is the dimension of Alice's sub-system,  $S(\rho)$  is the von-Neumann entropy of the state  $\rho$ , and qubit A is with Alice and B is with Bob.

## 6.1 Three-Qubit States as Quantum Channels for Dense Coding

For analysing the efficiencies of partially entangled three-qubit states for dense coding protocol, we assume that the first two qubits are with Alice and the last qubit is with Bob. For a maximally entangled  $|\Phi\rangle$  or GHZ state, Alice can send three bits of classical information, as she can in principle generate eight distinct orthogonal basis states by performing eight different operations on her two qubits. However, for the standard  $W$  state as a quantum channel, Alice can only send 2.91831 bits of information to Bob. We now proceed to analyse how the efficiencies of different partially entangled states stand for the dense coding protocol.

### 6.1.1 $|\Phi\rangle$ State as a Quantum Channel

The dense coding capacity given by (16) using a  $|\Phi\rangle$  state as a quantum channel is evaluated to be 3. This indicates that, under ideal conditions, one can use any  $|\Phi\rangle$  state for maximum information transfer. For actual evaluation, considering decoherence similar to the teleportation case, the dense coding capacity of the  $|\Phi\rangle$  states decreases under noisy conditions (see Fig. 12a). For example, the  $|\Phi\rangle$  states are not useful for dense coding protocol for  $d > 0.2$ .

Figure 12b demonstrates the effect of weak measurement and its reversal operations on the dense coding capacity, considering  $d = 0.5$ . Clearly, the dense coding capacity exceeds the classical bound whenever  $w \geq 0.6$  for a given range of parameters. At higher values of  $w$ , the dense coding capacity is always better than that of the classical one. The increase in dense coding capacity, however, decreases with the value of the state parameter, indicating that, if the originally prepared states are less entangled, one will obtain better results in dense coding protocol under noisy conditions.

### 6.1.2 GGHZ State as a Quantum Channel

The dense coding capacity of GGHZ states as resources in ideal condition is given as

$$C = \log_2(4) - \cos^2 \theta^2 \log_2(\cos^2 \theta^2) - \sin^2 \theta^2 \log_2(\sin^2 \theta^2). \quad (17)$$

Figure 13a and b describe the effect of the amplitude damping channel and weak measurement and its reversal

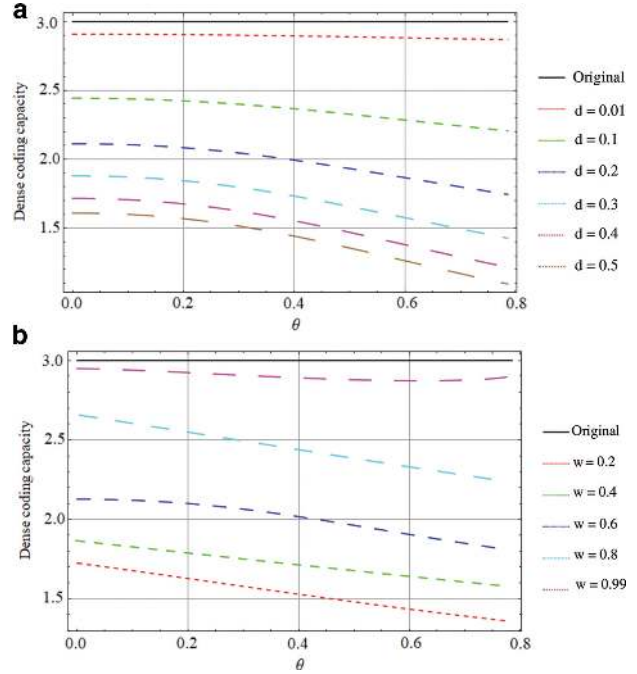


**Figure 12:** Effect of decoherence and weak measurement on the  $|\Phi\rangle$  state: (a) represents the loss of dense coding capacity when all three qubits of the  $|\Phi\rangle$  state undergo decoherence ( $d_1 = d_2 = d_3 = d$ ); (b) represents improving dense coding capacity in decoherence environment ( $d = 0.5$ ) using weak measurement on all three qubits of the  $|\Phi\rangle$  state ( $w_1 = w_2 = w_3 = w$ ).

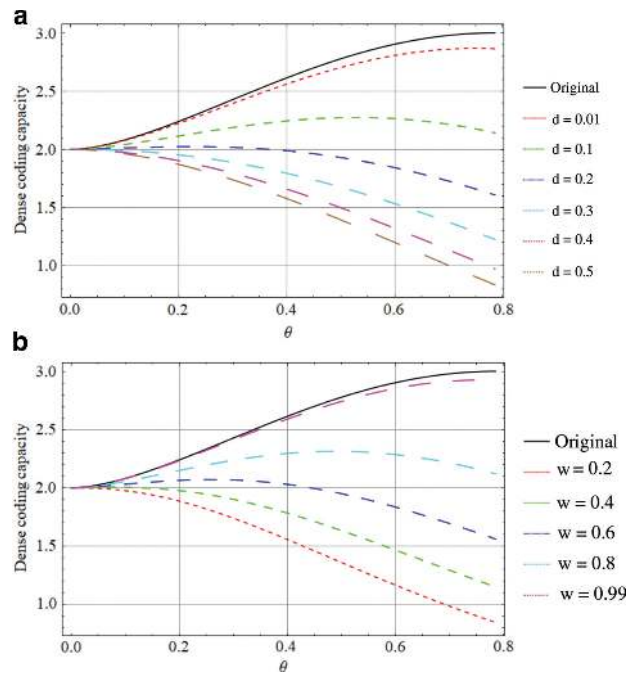


**Figure 13:** Effect of decoherence and weak measurement on the GGHZ state: (a) represents the loss of dense coding capacity when all three qubits of the GGHZ state undergo decoherence ( $d_1 = d_2 = d_3 = d$ ); (b) represents improving dense coding capacity in decoherence environment ( $d = 0.5$ ) using weak measurement on all three qubits of the GGHZ state ( $w_1 = w_2 = w_3 = w$ ).

operations on dense coding capacity, respectively. Similar to the  $|\Phi\rangle$  states, in the decoherence environment, the dense coding capacity falls below the classical limit for  $d \geq 0.2$ . On application of weak measurement and its reversal operations, the dense coding capacity regains its quantum advantages for  $w > 0.6$ . Like the teleportation scenario, in this case also the dense coding capacity above the classical bound increases with the state parameter, attains a maximum value, and then decreases again. Similarly, if we compare the efficiencies of  $|\Phi\rangle$  and GGHZ states under noisy conditions, we find that for lower (higher) values of the state parameter  $\theta$ ,  $|\Phi\rangle$  (GGHZ) states are more robust in comparison to the GGHZ ( $|\Phi\rangle$ ) states. For example, if we consider the decoherence parameter  $d = 0.5$ , then for  $\theta \leq 0.54$ , the  $|\Phi\rangle$  states are better resources than the GGHZ states, whereas for  $\theta > 0.54$ , the GGHZ states are better resources than the  $|\Phi\rangle$  states.

### 6.1.3 $W$ state as a Quantum Channel

In this case, the dense coding capacity is given by

$$C = \log_2(4) - \cos^2 \theta \log_2(\cos^2 \theta) - \sin^2 \theta \log_2(\sin^2 \theta). \quad (18)$$

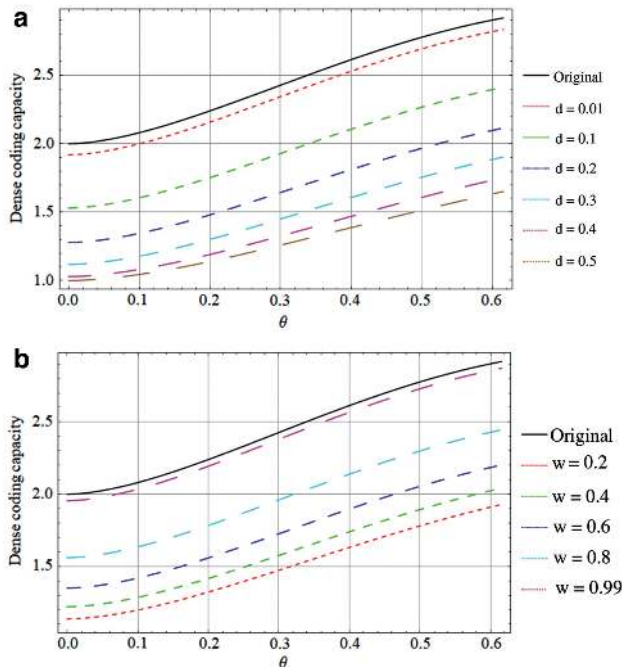


**Figure 14:** Effect of decoherence and weak measurement on the  $W$  state: (a) represents loss of dense coding capacity when all three qubits of the  $W$  state undergo decoherence ( $d_1 = d_2 = d_3 = d$ ); (b) represents improving dense coding capacity in decoherence environment ( $d = 0.5$ ) using weak measurement on all three qubits of the  $W$  state ( $w_1 = w_2 = w_3 = w$ ).

Figure 14a and b describe the effect of amplitude damping decoherence and weak measurement and its reversal operations on the dense coding capacity using  $W$  states as a quantum channel. A comparison of dense coding efficiencies for the three states indicates that  $|\Phi\rangle$  and GGHZ states are more robust towards noise for the dense coding protocol in comparison to  $W$  states. Within the class of  $W$  states, weak measurements and its reversal operations enhance the dense coding capacity, which increases with the state parameter as well. Similar to teleportation, at  $\theta = 35.2644^\circ$ , the standard  $W$  states are more efficient than the  $|\Phi\rangle$  and GGHZ states for certain values of the weak measurement parameter (say  $w = 0.6$ ).

## 7 Efficiency of Partially Entangled States in Noisy Conditions Using Non-optimum Weak Measurement Operations

The optimum value of the weak measurement reversal strength that leads to the effective enhancement in the efficiencies of quantum information processing protocols, as discussed above, is given by  $w_r = w + d(1 - w)$  [59]. In this section, we raise the question of using non-optimal weak measurement reversal operations: namely is it possible to obtain better efficiency in a protocol using non-optimal reversal operations in comparison to the use of optimal reversal operations? Interestingly, our results show that for a given decoherence parameter, fixing the value of the weak measurement parameter (or  $w_r$ ) results in the fidelity or dense coding capacity to be equal to the fidelity or dense coding capacity that can be obtained using a maximally entangled pure state. For example, using the GGHZ state as a quantum channel, at  $d = 0.5$  and  $w = 0.8$ , one can achieve fidelity close to unity for the values of  $w_r = 0.99$  and  $\theta = 0.029$  (Figs. 15a and 16a). In addition, if we first fix  $w_r = 0.99$ , then for the value of decoherence parameter  $d = 0.5$ , the use of partially entangled GGHZ states as resources results in very high average teleportation fidelity at very small values of the state parameter ( $\theta \in [0.003, 0.4]$ ), for all values of the weak measurement strength below  $w = 0.98$ . Similarly, for dense coding protocol also one can transfer 2.87 bits of message using Alice's 2 qubits for the same values of the parameters (Figs. 15b and 16b).

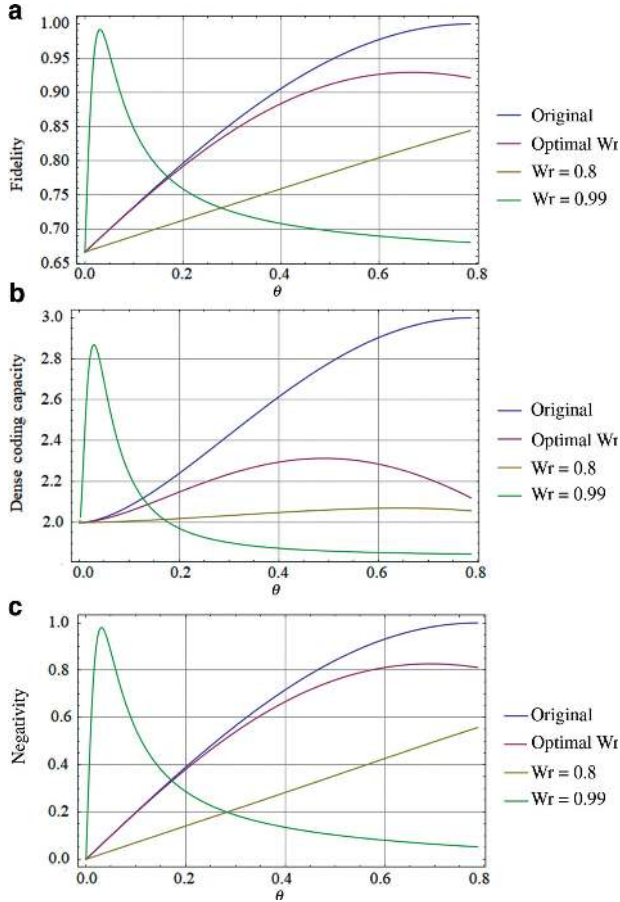


**Figure 15:** (a) Average teleportation fidelity, (b) dense coding capacity, and (c) negativity for the GHZ state when the decoherence parameter  $d = 0.5$  and weak measurement strength  $w = 0.8$ .

For studying the efficiencies of mixed states evolving from the initially prepared GHZ states for non-optimal weak measurement strengths at different values of state parameters, we characterise the degree of entanglement in these states using tripartite negativity [74] as a measure of entanglement for mixed states, which is defined as

$$N(\rho_{ABC}) = \sqrt[3]{N(\rho^{T_A})N(\rho^{T_B})N(\rho^{T_C})}, \quad (19)$$

where  $N(\rho^{T_i}) = -2\lambda_{\text{neg}}$ ,  $\lambda_{\text{neg}}$  is sum of negative eigenvalues of  $\rho^{T_i}$ , and  $\rho^{T_i}$  is partial transpose of  $\rho_{ABC}$  with respect to sub-system  $i$ . Clearly for  $\theta = 0.029$ , the value for tripartite negativity is very high (see Figs. 15c and 16c), and therefore the degree of entanglement of the finally shared state justifies the efficiency of these states at the lower value of the state parameter.

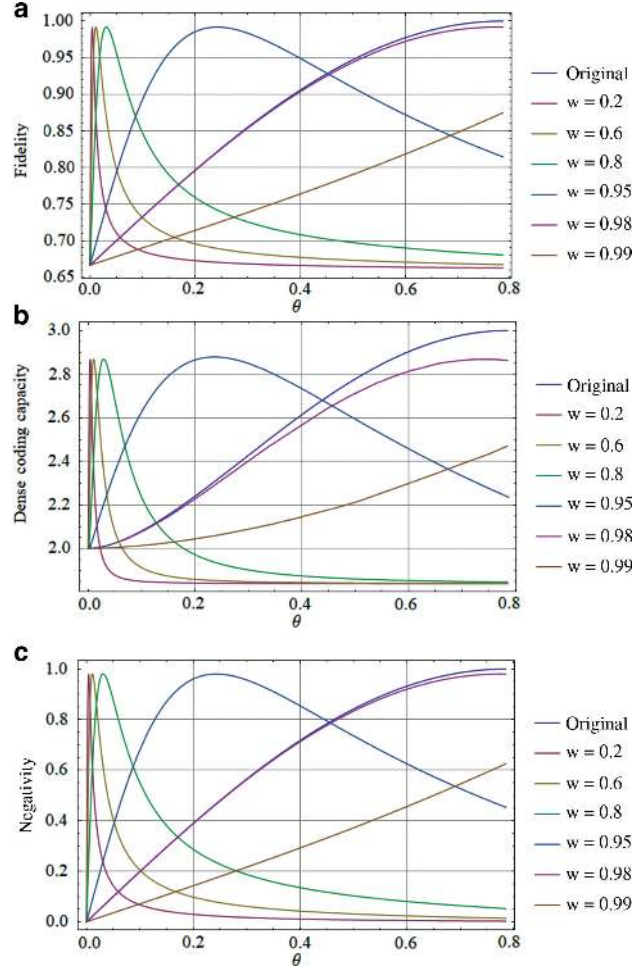


**Figure 16:** (a) Average teleportation fidelity, (b) dense coding capacity, and (c) negativity for the GHZ state when decoherence parameter  $d = 0.5$  and reversal weak measurement strength  $w_r = 0.99$ .

## 8 Summary and Conclusion

In any quantum information processing protocol, it is imperative to analyse the efficacy of entangled resources under real conditions. In fact, in any actual set-up avoiding the interaction of qubits with the environment may not be feasible, and hence one needs to study models that lead to real conditions such that maximum efficiency can be achieved and the associated parameters and their effects on the protocol can be understood. Therefore, in the present study, we have analysed the efficiency of three-qubit partially entangled states in two inequivalent classes of three-qubit entangled states in presence of noise and applications of weak measurement and its reversal operations. Our results indicate that, for teleportation protocol, the  $|\Phi\rangle$  states are more robust to decoherence for smaller

values of the parameter  $\theta$  in comparison to the GHZ states. However, efficiency of the GHZ states exceeds that of the  $|\Phi\rangle$  states once  $\theta$  exceeds a certain value. For example, when decoherence is 0.5 and the state parameter  $\theta \leq \frac{\pi}{9}$  ( $= 0.35$ ), the states  $|\Phi\rangle$  are more efficient for teleportation in comparison to the GHZ states, whereas for  $\theta > \frac{\pi}{9}$ , the GHZ states are more efficient. Moreover, the efficiencies of  $|\Phi\rangle$  and GHZ states are found to be more robust in comparison to  $W$  states in the presence of noise. Interestingly, standard  $W$  states are found to be more efficient in comparison to  $|\Phi\rangle$  and GHZ states for small values of the weak measurement strength parameter. In all three cases, we found that fidelity of teleportation increases with the strength of weak measurement and its reversal operations irrespective of the value of decoherence parameter. For very high values of the weak measurement strength parameter, the  $|\Phi\rangle$  states lead to unit fidelity irrespective of the values of noise and state parameters. For dense coding protocol, we found similar results as in the case of quantum teleportation. Further, we observed degradation in dense coding capacity with increase in decoherence and enhancement in capacity with the application of weak measurement and its reversal operations. We further characterised the efficiencies of these states in terms of quantum correlations originating from the Svetlichny inequality and global quantum discord. Our analysis raises a question regarding the effectiveness of the Svetlichny inequality in capturing quantum correlations in an underlying quantum state. Interestingly, or rather surprisingly, although the geometric discord of the finally shared states under decoherence is more if the initially prepared  $|\Phi\rangle$  or GHZ state is maximally entangled, the efficiency of the initially prepared partially entangled  $|\Phi\rangle$  or GHZ states for teleportation and dense coding is found to be better than the efficiency of maximally entangled states. Therefore, in contrast to the general belief that more correlations may lead to better efficiency, in this study we found that less correlations can be more useful for certain protocols as well, provides another proof for the complex nature of multi-qubit entanglement. We also found that when we apply non-optimum reversing weak measurement, for a specific value of the state parameter  $\theta$ , the partially entangled GHZ state is more efficient for quantum protocols than all other states of the same class. Hence, the study presented here provides an efficient method to select appropriate entangled resources for quantum information processing protocols depending on the decoherence parameter as well as the weak measurement and its reversal strength parameter.

**Acknowledgements:** The authors thank the Ministry of Human Resource Development (MHRD), Government of India, and IIT Jodhpur for providing the research facility.

## References

- [1] C. H. Bennett and D. P. DiVincenzo, *Nature* **404**, 247 (2000).
- [2] N. Gisin, G. Ribordy, W. Tittel, and H. Zbinden, *Rev. Mod. Phys.* **74**, 145 (2002).
- [3] C. H. Bennett, G. Brassard, C. Crépeau, R. Jozsa, A. Peres, et al., *Phys. Rev. Lett.* **70**, 1895 (1993).
- [4] C. H. Bennett and S. J. Wiesner, *Phys. Rev. Lett.* **69**, 2881 (1992).
- [5] M. Hillery, V. Bužek, and A. Berthiaume, *Phys. Rev. A* **59**, 1829 (1999).
- [6] A. Einstein, B. Podolsky, and N. Rosen, *Phys. Rev.* **47**, 777 (1935).
- [7] J. S. Bell, *Phys. Phys. Fiz.* **1**, 195 (1964).
- [8] A. Aspect, P. Grangier, and G. Roger, *Phys. Rev. Lett.* **47**, 460 (1981).
- [9] A. Aspect, P. Grangier, and G. Roger, *Phys. Rev. Lett.* **49**, 91 (1982).
- [10] A. Aspect, J. Dalibard, and G. Roger, *Phys. Rev. Lett.* **49**, 1804 (1982).
- [11] I. Chuang and M. Nielsen, *Quantum Computation and Quantum Information*, Cambridge University Press, New York, NY, 2010.
- [12] W. H. Zurek, *Rev. Mod. Phys.* **75**, 715 (2003).
- [13] M. P. Almeida, F. de Melo, M. Hor-Meyll, A. Salles, S. P. Walborn, et al., *Science* **316**, 579 (2007).
- [14] A. R. R. Carvalho, F. Mintert, and A. Buchleitner, *Phys. Rev. Lett.* **93**, 230501 (2004).
- [15] M. Hein, W. Dür, and H.-J. Briegel, *Phys. Rev. A* **71**, 032350 (2005).
- [16] M. Mahdian, R. Yousefjani, and S. Salimi, *Eur. Phys. J. D* **66**, 133 (2012).
- [17] M. Tchoffo, L. T. Kenfack, G. C. Fouokeng, and L. C. Fai, *Eur. Phys. J. Plus* **131**, 380 (2016).
- [18] A. Acin, T. Durt, N. Gisin, and J. I. Latorre, *Phys. Rev. A* **65**, 052325 (2002).
- [19] A. A. Méthot and V. Scarani, arXiv preprint quant-ph/0601210 (2006).
- [20] B. C. Hiesmayr, *Eur. Phys. J. C* **50**, 73 (2007).
- [21] N. Brunner, *Phys. E: Low Dimens. Syst. Nanostruct.* **42**, 354 (2010).
- [22] M. Junge and C. Palazuelos, *Commun. Math. Phys.* **306**, 695 (2011).
- [23] T. Vidick and S. Wehner, *Phys. Rev. A* **83**, 052310 (2011).
- [24] R. Chaves, A. Acn, L. Aolita, and D. Cavalcanti, *Phys. Rev. A*, **89**, 042106 (2014).
- [25] A. de Rosier, J. Gruca, F. Parisio, T. Vértesi, and W. Laskowski, *Phys. Rev. A* **96**, 012101 (2017).
- [26] P. Singh and A. Kumar, *Quantum Inf. Process.* **17**, 249 (2018).
- [27] P. Singh and A. Kumar, *Z. Naturforsch. A* **73**, 191 (2018).
- [28] P. Singh and A. Kumar, *Int. J. Theor. Phys.* **57**, 3172 (2018).
- [29] E. A. Fonseca and F. Parisio, *Phys. Rev. A* **92**, 030101 (2015).

- [30] S.-W. Lee and D. Jaksch, *Phys. Rev. A* **80**, 010103 (2009).
- [31] S.-W. Ji, J. Lee, J. Lim, K. Nagata, and H.-W. Lee, *Phys. Rev. A* **78**, 052103 (2008).
- [32] A. Karlsson and M. Bourennane, *Phys. Rev. A* **58**, 4394 (1998).
- [33] P. Agrawal and A. Pati, *Phys. Rev. A* **74**, 062320 (2006).
- [34] F. L. Yan, T. Gao, and Y. C. Li, *Europhys. Lett.* **84**, 50001 (2008).
- [35] E. Jung, M.-R. Hwang, Y. H. Ju, M.-S. Kim, S.-K. Yoo, et al., *Phys. Rev. A* **78**, 012312 (2008).
- [36] M. Y. Wang and F. L. Yan, *Eur. Phys. J. D* **54**, 111 (2009).
- [37] W.-L. Li, C.-F. Li, and G.-C. Guo, *Phys. Rev. A* **61**, 034301 (2000).
- [38] S. Popescu, *Phys. Rev. Lett.* **72**, 797 (1994).
- [39] C. H. Bennett, G. Brassard, S. Popescu, B. Schumacher, J. A. Smolin, et al., *Phys. Rev. Lett.* **76**, 722 (1996).
- [40] R. Horodecki, M. Horodecki, and P. Horodecki, *Phys. Lett. A* **222**, 21 (1996).
- [41] M.-L. Hu, *Phys. Lett. A* **375**, 922 (2011).
- [42] P. Espoukheh and P. Pedram, *Quantum Inf. Process.* **13**, 1789 (2014).
- [43] T. Hiroshima, *Phys. Lett. A* **301**, 263 (2002).
- [44] J.-W. Pan, S. Gasparoni, R. Ursin, G. Weihs, and A. Zeilinger, *Nature* **423**, 417 (2003).
- [45] P. G. Kwiat, A. J. Berglund, J. B. Altepeter, and A. G. White, *Science* **290**, 498 (2000).
- [46] S. Maniscalco, F. Francica, R. L. Zaffino, N. L. Gullo, and F. Plastina, *Phys. Rev. Lett.* **100**, 090503 (2008).
- [47] P. W. Shor, *Phys. Rev. A* **52**, R2493 (1995).
- [48] X. Xiao, Y. Yao, W.-J. Zhong, Y.-L. Li, and Y.-M. Xie, *Phys. Rev. A* **93**, 012307 (2016).
- [49] A. N. Korotkov and K. Keane, *Phys. Rev. A* **81**, 040103 (2010).
- [50] X. Xiao and Y.-L. Li, *Eur. Phys. J. D* **67**, 204 (2013).
- [51] Y. W. Cheong and S.-W. Lee, *Phys. Rev. Lett.* **109**, 150402 (2012).
- [52] Q. Sun, M. Al-Amri, and M. S. Zubairy, *Phys. Rev. A* **80**, 033838 (2009).
- [53] G. S. Paraoanu, *Phys. Rev. Lett.* **97**, 180406 (2006).
- [54] R. L. Franco, B. Bellomo, E. Andersson, and G. Compagno, *Phys. Rev. A* **85**, 032318 (2012).
- [55] N. Katz, M. Neeley, M. Ansmann, R. C. Bialczak, M. Hofheinz, et al., *Phys. Rev. Lett.* **101**, 200401 (2008).
- [56] Q. Sun, M. Al-Amri, L. Davidovich, and M. S. Zubairy, *Phys. Rev. A* **82**, 052323 (2010).
- [57] G. S. Paraoanu, *Phys. Rev. A* **83**, 044101 (2011).
- [58] J.-C. Lee, Y.-C. Jeong, Y.-S. Kim, and Y.-H. Kim, *Opt. Express* **19**, 16309 (2011).
- [59] Y.-S. Kim, J.-C. Lee, O. Kwon, and Y.-H. Kim, *Nat. Phys.* **8**, 117 (2012).
- [60] A. N. Korotkov and A. N. Jordan, *Phys. Rev. Lett.* **97**, 166805 (2006).
- [61] Y.-S. Kim, Y.-W. Cho, Y.-S. Ra, and Y.-H. Kim, *Opt. Express* **17**, 11978 (2009).
- [62] X.-Y. Xu, Y. Kedem, K. Sun, L. Vaidman, C.-F. Li, et al., *Phys. Rev. Lett.* **111**, 033604 (2013).
- [63] N. Katz, M. Ansmann, R. C. Bialczak, E. Lucero, R. McDermott, et al., *Science* **312**, 1498 (2006).
- [64] J. P. Groen, D. Ristè, L. Tornberg, J. Cramer, P. C. De Groot, et al., *Phys. Rev. Lett.* **111**, 090506 (2013).
- [65] S.-Y. Guan, Z. Jin, H.-J. Wu, A.-D. Zhu, H.-F. Wang, et al., *Quantum Inf. Process.* **16**, 137 (2017).
- [66] T. Pramanik and A. S. Majumdar, *Phys. Lett. A* **377**, 3209 (2013).
- [67] W. Dür, G. Vidal, and J. I. Cirac, *Phys. Rev. A* **62**, 062314 (2000).
- [68] G. Svetlichny, *Phys. Rev. D* **35**, 3066 (1987).
- [69] C. C. Rulli and M. S. Sarandy, *Phys. Rev. A* **84**, 042109 (2011).
- [70] S. Oh, S. Lee, and H.-W. Lee, *Phys. Rev. A* **66**, 022316 (2002).
- [71] L. T. Knoll, C. T. Schmiegelow, and M. A. Larotonda, *Phys. Rev. A* **90**, 042332 (2014).
- [72] S. Massar and S. Popescu, *Phys. Rev. Lett.* **74**, 1259 (1995).
- [73] G. Bowen, *Phys. Rev. A* **63**, 022302 (2001).
- [74] C. Sabn and G. Alcaine, *Eur. Phys. J. D* **48**, 435 (2008).